water

MDPI

Article

The Influence of Non-Pressure Pipes Filled to Different Degrees on the Hydraulic Characteristics of Channel–Pipe Combined Irrigation Systems

Xiaomeng Jia [1,2,*], Wenzheng Zhang [1,2], Yingying Wang [1,2], Yuqi Shen [1,2] and Yi Sun [1,2]

[1] Farmland Irrigation Research Institute, Chinese Academy of Agricultural Sciences, Xinxiang 453002, China; zhangwenzheng@caas.cn (W.Z.); wangyingying01@caas.cn (Y.W.); 17634755765@163.com (Y.S.); sun20000706@163.com (Y.S.)
[2] Key Laboratory of Water Saving Irrigation Engineering, Ministry of Agriculture and Rural Affairs, Xinxiang 453002, China
* Correspondence: jiaxiaomeng0065@163.com; Tel.: +86-136-2367-0626

Abstract: Modern irrigation areas often use a combination of channels and pipes for irrigation. Due to changes in terrain, inflow, and pipe diameter, pipelines are often prone to experiencing a state of no pressure. This lack of pressure affects not only the velocity distribution and water surface profile of the main channel but also the velocity distribution and flow distribution of the pipeline. Therefore, in this study, we employed a combination of physical model experiments and theoretical analysis to study the influence of non-pressure pipelines on the hydraulic characteristics of channel–pipe combined irrigation systems filled to different degrees. Through this, the variation laws of the flow velocity distribution, turbulence intensity, water surface, diversion width, and diversion ratio under different filling degrees were obtained. The non-pressure pipeline flow velocity expression was obtained through dimensional analysis, and the calculation formula for the non-pressure pipeline flow velocity coefficient was fitted using linear regression analysis. The relative error between the calculated value and the measured value did not exceed 8.81%. The research results presented in this article can provide technical support for the design and maintenance of channel–pipe combined irrigation systems.

Keywords: farmland irrigation; channel–pipe combination; hydraulic characteristics; filling degrees; non-pressurized

check for updates

Citation: Jia, X.; Zhang, W.; Wang, Y.; Shen, Y.; Sun, Y. The Influence of Non-Pressure Pipes Filled to Different Degrees on the Hydraulic Characteristics of Channel–Pipe Combined Irrigation Systems. *Water* **2024**, *16*, 3449. https://doi.org/10.3390/w16233449

Academic Editor: Giuseppe Pezzinga

Received: 21 October 2024
Revised: 24 November 2024
Accepted: 28 November 2024
Published: 30 November 2024

Copyright: © 2024 by the authors. Licensee MDPI, Basel, Switzerland. This article is an open access article distributed under the terms and conditions of the Creative Commons Attribution (CC BY) license (https://creativecommons.org/licenses/by/4.0/).

1. Introduction

As a major agricultural country, China has a long history of irrigated agriculture, and the scarcity of water resources has always been an important factor restricting agricultural development [1]. Therefore, determining how to improve the utilization rate of irrigation water and promote the sustainable development of agricultural water systems has become a critical issue that urgently needs to be solved [2]. Compared to water delivery via channels, water delivery via pipes saves more water and offers advantages such as reducing land use, facilitating construction management, preventing water pollution, and integrating agricultural machinery and irrigation [3]. Therefore, adapting to local conditions and gradually realizing the use of pipes instead of channels for irrigation constitute an inevitable trend in the development of modern water-saving irrigation areas [4,5]. However, in the process of renovating water-saving systems in irrigation areas, achieving simultaneous full channel channelization requires a relatively large capital investment. Notably, regions such as Europe, America, and Japan, which have highly developed irrigation technologies, are also gradually promoting channelization. At the same time, considering China's current levels of economic development and irrigation area research, it has been found that adopting a channel–pipe combined irrigation system for water delivery is both reasonable and urgent from a modern perspective [6].

Channel–pipe combined irrigation systems have been widely applied around the world [7–11]. Since the 1960s, Japan has been using a channel–pipe combined irrigation system, and it has successively transformed the pipelines of channels below the branch channels in irrigation areas, allowing a transformation from single-stage channels to pipelines, multi-stage pipelines, and, finally, a pipeline network [12]. In the mid-1980s, the Soviet Union diverted water from channels through pipelines and then distributed it to farmland for irrigation through buried pipeline systems. The San Joaquin Valley irrigation district in California had already transformed the channels below its main canal into pipelines for water supply and irrigation by the end of the last century. In the process of channel channelization, Israel has gradually integrated and connected its main water systems and built an interconnected system of surface, underground, and return water, which has facilitated the unified management of agricultural water use in the country [13]. In China, some self-flowing irrigation areas directly use pipelines instead of some channels for water transportation and irrigation. In hilly areas, the "long vine and melon" irrigation method is commonly used; it involves introducing water into a reservoir and then using pipes to bring the water into a field. This water supply model effectively enhances the adaptability of channel–pipe combined irrigation systems to the terrain. In response to the problem of high sediment content in water sources in northern irrigation areas, a study was conducted on the hydraulic characteristics of channel–pipe combined irrigation systems under sediment-rich conditions, providing a theoretical basis for rational pipeline renovation in northern channel irrigation areas [14–16]. In addition, accelerating the research and development of low-cost, large-diameter, high-quality pipe materials; strengthening the design optimization of channel–pipe combined irrigation systems; and formulating corresponding technical specifications for channel–pipe combined irrigation systems have become the main research directions for many scholars [17,18].

In the construction and renovation process in modern irrigation areas, large-diameter pipelines are widely used, and due to factors such as terrain and water inflow, non-pressurized pipe flow often occurs. Compared to pressurized pipe flow, the flow field distribution of non-pressurized pipe flow is more complex, and the changes in the flow field will have an impact on the flow distribution, water delivery efficiency, and stable operation of the system. Therefore, it is necessary to strengthen the research on the hydraulic characteristics of channel–pipe combined irrigation systems under non-pressurized pipe flow conditions. Numerous scholars have conducted research on non-pressurized pipe flow [19–22]. White studied the hydraulic parameters related to uniform flow in non-pressure pipes based on the Chezy and Manning formulas [23]. Through research, Knight found that the maximum velocity value of the cross-section under non-full-pipe conditions occurs below the horizontal plane, and the location of the maximum velocity point is mainly affected by the filling degree, roughness, and lateral position [24]. Yoon measured the three-dimensional velocity of non-pressure pipe flow and obtained the velocity formula and wall friction coefficient using a nonlinear least-squares fitting method [25]. Jiang found that the flow velocity near the pipe wall in a non-pressurized pipe state is mainly affected by the friction force of the pipe wall and the slope of the bottom of the pipe, but near the free water surface, the flow velocity distribution is mainly affected by the contraction of the pipe wall and secondary flow [26]. Mohamed studied the critical and normal water depths of non-uniform flow in non-pressure pipes and provided new approximate calculation formulas for both [27]. Mao Zeyu explored the non-singular relationship between a uniform flow rate and filling degree in non-pressure pipes and proposed a simpler expression for flow velocity calculation [28]. Ding Falong studied the distribution patterns of cross-sectional flow velocity, wall shear stress, and Reynolds shear stress in non-pressure pipelines through numerical simulations [29].

Research on non-pressure pipe flow is mostly focused on a single complete pipeline, and there is relatively little research on the hydraulic characteristics of channel–pipe combined irrigation systems under non-pressure pipe conditions. Therefore, this study aims to address the common problem of non-pressure pipe flow in irrigation channel–pipe

combined irrigation systems, a relatively rare focus in the existing research. A combination of model experiments and theoretical analysis was used to study the flow velocity distribution, turbulence intensity, water surface changes, diversion width, diversion ratio, and other issues affecting the main channel under different filling degrees. Dimensional analysis was used to derive the expression for non-pressure pipe flow velocity. The research content of this article can further improve the theoretical basis of channel–pipe combined irrigation systems and provide technical support for the modernization and renovation of irrigation areas.

2. Materials and Methods

2.1. Experimental System

The experimental system mainly included three parts: a power system, a regulation system, and a testing system. The power system was mainly composed of centrifugal pumps. The regulation system mainly included regulating valves and electric gates. The testing system included a water-level-measuring needle, an acoustic Doppler velocimeter, an electromagnetic flowmeter, and a non-pressure pipe electromagnetic flowmeter. The main channel in this experiment was composed of transparent glass and an iron frame with an inner width of 58 cm, a depth of 60 cm, and a length of 2100 cm. A pipe was drilled into the side wall of the channel at a certain distance from the entrance of the main channel (where the water flow in the channel is basically stable); the wall material was organic glass. The inner diameter of the pipe was 10 cm, and the distance from the center of the pipe to the bottom of the channel was 15 cm. It was connected in sections by flanges, and support devices were installed below the pipe at regular intervals. A schematic diagram of the experimental system is shown in Figure 1.

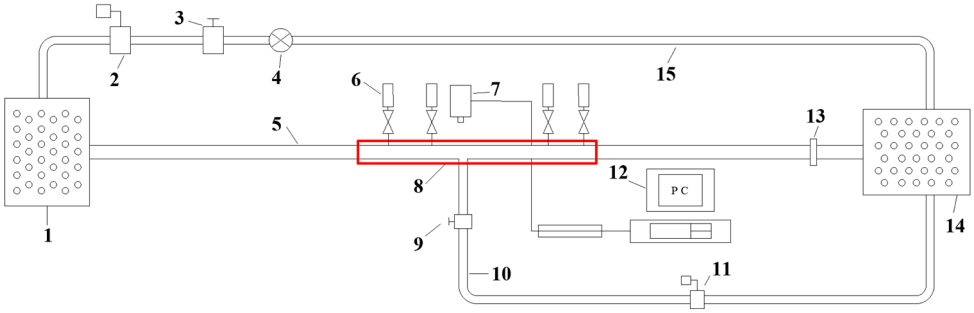


Figure 1. Experimental system. Note: 1. water tank; 2. centrifugal pump; 3. regulating valve; 4. electromagnetic flowmeter; 5. main channel; 6. water-level-measuring needle; 7. acoustic Doppler velocimeter; 8. test section; 9. gate valve; 10. pipe; 11. non-pressure pipe electromagnetic flowmeter; 12. computer; 13. electric gate; 14. underground reservoir; 15. return water pipeline.

Before the start of the test, the electric gate at the end of the main channel was adjusted to the appropriate opening, and then the water from the underground reservoir was pumped into the water tank by a centrifugal pump, and the flow rate was adjusted using the regulating valve and an electromagnetic flowmeter. When the water depth in the water tank reaches a certain level, the water flows into the main channel; with the continuous increase in the depth of the water in the main channel, the water flows into the pipe. A scale was installed on the wall of the experimental channel. Different filling degrees in the pipeline correspond to different scales. After the experiment began, the water depth in the channel was changed via the regulating valve. When the water depth reached the corresponding scale, the water flow in the pipeline reached the required filling degree for the experiment. At this point, the pipeline was not completely filled with water, leading to a non-pressurized pipeline. When the flow of water in the main channel and pipeline was stable, an acoustic Doppler velocimeter was used to measure the water flow velocity at different depths in the main channel, and a water-level-measuring needle was used to measure the water depth at corresponding locations in the main channel. A non-pressure

pipe electromagnetic flowmeter was installed on the pipeline to measure the flow rate inside the pipe. The experimental devices and instruments are shown in Figure 2.

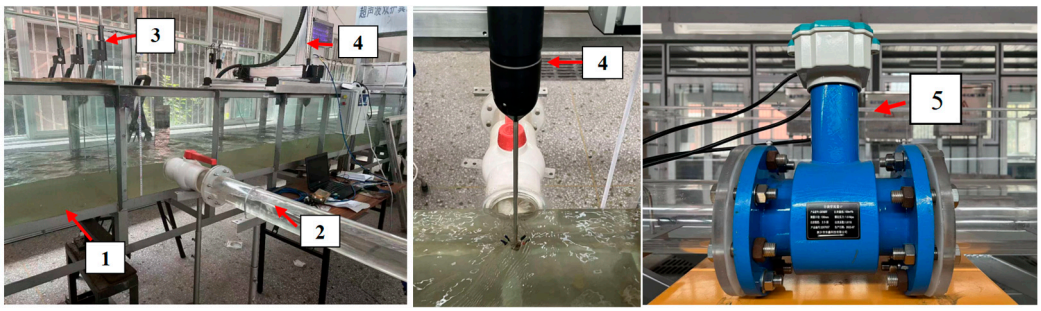


Figure 2. Experimental devices and instruments. Note: 1. main channel; 2. pipe; 3. water-level-measuring needle; 4. acoustic Doppler velocimeter; 5. non-pressure pipe electromagnetic flowmeter.

An acoustic Doppler velocimeter (ADV, Nortek Vectrino, manufactured by Nortek AS in Rud, Norway) was used to measure cross-sectional flow velocity. The smallness of the flowmeter probe reduces any interference it could cause. During flow measurement, the probe was submerged in water for data collection, and the parameters of the flowmeter were set through a computer. The ADV's sampling volume is 7.0, its transmission length is 1.8, and its average signal-to-noise ratio is 15 dB. The flow velocity measurement frequency was set to 200 Hz, with a sampling time of 5 s, and a total of 1000 instantaneous flow velocity values were obtained at each measurement point. In order to reduce the impact of probe movement on instantaneous flow velocity and improve the reliability of the sampling data, the measured data were screened, and those with an average signal-to-noise ratio greater than 15 dB and a correlation coefficient greater than 90% were selected. The water flow may appear as bubbles—impurities caused by the influence of the external environment. These issues show up as burrs in the time series. The speed threshold method was used to replace data that were not within the threshold, ultimately allowing data for computational analysis to be obtained. The water depth was measured using the SCM60 water-level-measuring needle, with an accuracy of ± 0.1 mm.

The velocity values collected by the acoustic Doppler flowmeter used in the experiment are based on the three-dimensional velocity in a cartesian coordinate system. In order to facilitate the description of velocity changes in various directions, a corresponding cartesian coordinate system was established. The direction of water flow was defined as the positive x-axis direction, the positive y-axis direction was defined as the direction perpendicular to the water flow and pointing towards the side of the main channel wall where the pipe is located, and the positive z-axis direction was defined as the direction perpendicular to the bottom surface of the channel. The intersection point between the pipe centerline and the channel centerline at the bottom of the channel is the coordinate origin.

2.2. Experimental Scheme

For a non-pressure circular pipe, as the water depth inside the pipe changes, the shape of the cross-section of the flow also changes. The change in the cross-section of the flow will have an impact on the flow velocity distribution and water surface changes in the channel diversion zone. Therefore, we use the dimensionless constant Φ to reflect the changes in water depth inside the pipe. Φ represents the filling degree for the flow in the non-pressure pipe, which is the ratio of the water depth h in the pipe to the pipe diameter D. We selected three filling degrees in this experiment: 0.3, 0.5, and 0.8. During the experiment, the flow rate of the main channel remained constant, and the water depth in the main channel was changed by adjusting the opening of the electric gate, resulting in different filling degrees.

In order to intuitively reflect the pipe diversion situation of the main channel at different flow rates, the ratio of pipe flow Q_1 to incoming flow Q in the main channel is defined as the diversion ratio δ. The diversion ratio of the main channel flow was measured

under four conditions: 50 m^3/h, 70 m^3/h, 90 m^3/h, and 110 m^3/h. The opening of the electric valve at the end of the main channel remained unchanged. The centrifugal pump changed the flow rate inside the main channel, and the non-full pipe electromagnetic flowmeter measured the flow rate inside the pipe.

2.3. Cross-Section and Measurement Point Layout

In order to measure the flow velocity of the main channel, eleven transverse test cross-sections, #1 to 11, were set up from the upstream to downstream sections of the channel, as shown in Figure 3. Cross-sections #4~8 faced the inlet of the pipe, cross-section #6 was located at the center of the pipe, and cross-sections #7~11 and #1~5 were symmetrically distributed about cross-section #6. The distances between sections #1, #2, #3, #4, #5, and #6 were 25 cm, 15 cm, 8 cm, 5 cm, and 3 cm.

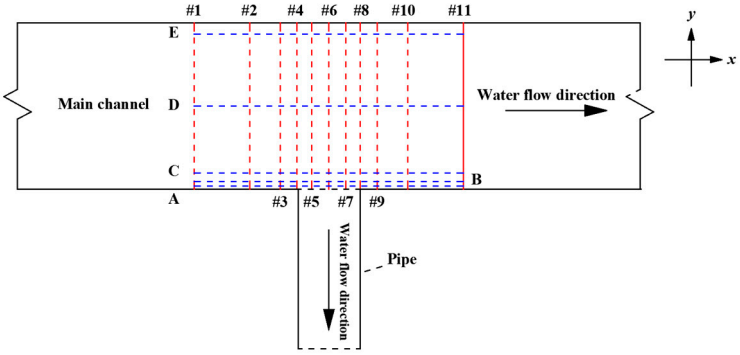


Figure 3. Cross-section layout. Note: #1~#11 represents cross-sections.

Due to the diversion effect of the pipe, the flow rate in the main channel would change, and the water surface along the main channel would also change accordingly. We set up 5 water level measurement lines in the main channel, corresponding to A~E in Figure 3. The intersection point between the water level measurement line and the transverse cross-section is a water level measurement point. Due to the disturbance of the pipe and the influence of wall shear stress, the water surface near the wall of the main channel on the side where the pipe was located is more complex. In order to accurately reflect the changes in the water surface at this location, three water surface measurement lines, A, B, and C, were arranged here, with a small distance maintained between the three water surface measurement lines. The distances between water surface measurement lines A~C and the main channel wall were 0.5 cm, 1 cm, and 4 cm. Water surface measurement line D was located at the center of the channel, and water surface measurement line 5 was 1 cm away from the main channel wall.

To measure the flow velocity of water at different depths, measurement lines were set up along the channel wall of the pipeline on each test section, with a total of 12 measurement lines, labeled I~XII. Water depth measurement line VII was located at the center of the main channel, and the distances from water depth measurement lines I~XII to the wall where the pipe was located were 2 cm, 4 cm, 6 cm, 11 cm, 17 cm, 23 cm, 29 cm, 38 cm, 44 cm, 50 cm, 53 cm, and 56 cm. Considering that the flow of water is greatly affected by the shear stress on the main channel wall, in order to accurately measure the flow velocity at the side walls of the main channel, we ensured the distance between the water-depth-measuring lines near the two side walls of the main channel was relatively small, and the distance between the water-depth-measuring lines in the middle area of the channel was relatively large due to the small influence of the main channel walls, as shown in Figure 4.

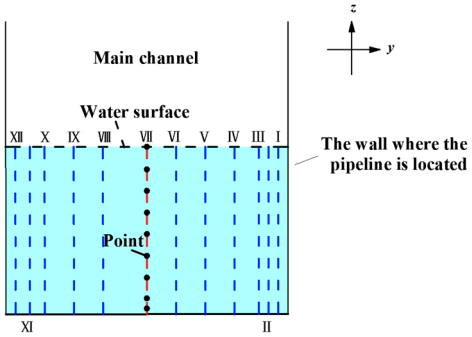


Figure 4. Layout of water depth measurement lines. Note: I~XII represents the measurement lines.

In order to accurately measure velocity at different filling degrees, measuring points were set up on each measuring line. We set up measuring points 1 cm away from the bottom of the channel towards the water surface, with a spacing of 2 cm between the measuring points. The locations of the measuring points at different filling degrees are shown in Table 1.

Table 1. Distribution of measuring points.

Φ	Distance between Measuring Point and Channel Bottom/cm	Total Number of Measuring Points per Cross-Section
0.3	1/3/5/7/9/11/13	84
0.5	1/3/5/7/9/11/13/15	96
0.8	1/3/5/7/9/11/13/15/17	108

3. Results

3.1. Analysis of the Flow Velocity of Channel–Pipe Combined Irrigation Systems

3.1.1. Analysis of Flow Velocity Distribution in the Main Channel

The distribution pattern of flow velocity along the main channel under different filling degrees was roughly the same throughout the experiments. We analyzed the variation in flow velocity along the main channel with a filling degree of 0.5 as an example. The variation in flow velocity with respect to water depth at each section of the main channel is shown in Figure 5. The horizontal and vertical axes in Figure 5 represent the relative velocity (v_i/v_a) and relative water depth (y/H). v_i/v_a is the ratio of the velocity of the measuring point to the average flow velocity of the channel water, and y/H is the ratio of the depth of the measuring point to the depth of the channel water.

The flow velocity distribution in the main channel can be divided into three regions, namely, the upstream (#1 and #2) and downstream regions (#10 and #11), which are less affected by the pipeline, and the regions (#3~9) that are more affected by the pipeline.

The flow velocity distribution in the upstream area of the main channel was relatively uniform. The cross-sectional water flow still maintained the distribution characteristics of open-channel water flow, and the flow velocity was logarithmically distributed from the bottom of the channel to the water surface. Due to the presence of wall shear stress, the water flow velocity near the bottom of the channel was relatively small, but the velocity gradient was large. Due to the influence of shear stress on the side wall of the main channel, the flow velocity value on measurement lines I and XII is lower than that on other measurement lines. Compared with other measuring lines, the flow velocity of measuring line I fluctuates greatly on the *x*-axis. The flow velocity values at the measuring points at the same depth on lines I and XII are approximately the same on cross-section #2. As the water flows toward the inlet of the pipeline, the velocity value on measurement line I continues to increase. The main reason for this is that as the flow of water gradually approaches the inlet of the pipeline, the water flowing near the channel wall tends to enter the pipeline. This part of the flow of water can be regarded as a curved water flow composed of uniform

flow in the channel and free outflow in the pipeline, leading to an increase in water flow velocity on measurement line I starting from section #3. Additionally, the flow velocity increases most significantly from the bottom of the pipeline to the water surface. When the water flow in the main channel reaches the upper edge of the pipeline (section #3), the streamline undergoes rapid bending, and the lateral velocity increases. Therefore, the flow velocity of measuring line I increases at sections #4–#6. The water flowing into the pipe is blocked by the downstream pipe wall, and the velocity of some regions of the flowing water decreases or even enters into reverse flow. This part of the water flow intersects with the incoming flow of the main channel, reducing the water flow velocity at section #8. Although section #9 is located downstream of the pipeline inlet, due to its proximity to the pipeline inlet, reverse water flow will form and converge into the pipeline. This reverse water flow intersects with the forward water flow in the main channel, resulting in a decrease in water flow velocity near section #9. The decrease in flow velocity values at each measuring point on section #10 is influenced by pipeline diversion, and due to the decrease in the influence of the pipeline inlet, the flow velocity along the water depth direction exhibits a logarithmic distribution.

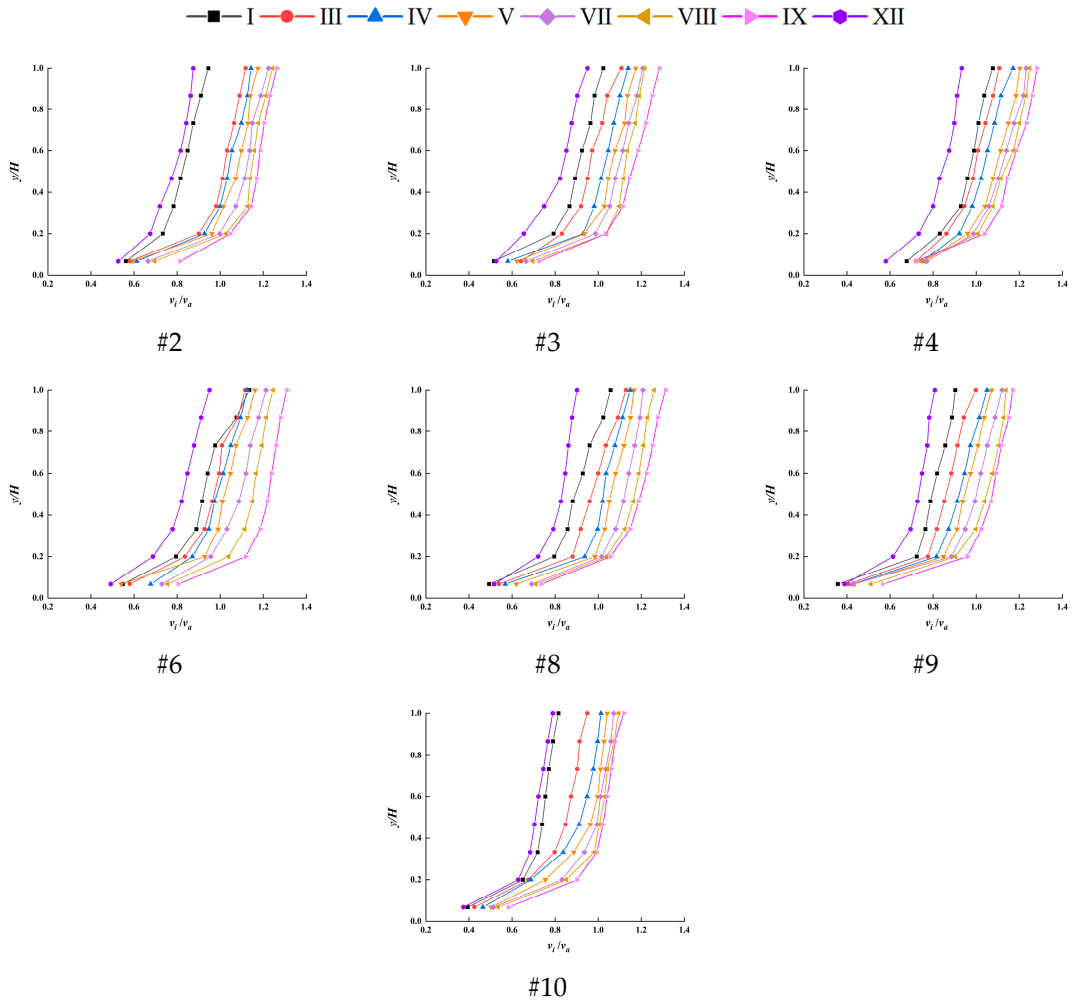


Figure 5. Variation in flow velocity with respect to water depth at each section when the filling degree was 0.5.

3.1.2. Turbulence Intensity

Turbulence intensity is a fundamental parameter of water flow turbulence performance, representing the fluctuation amplitude of instantaneous flow velocity. It is commonly expressed as the root mean square of pulsating flow velocity, as shown in Formula (1):

$$\sigma = \frac{\sqrt{\frac{1}{n}\sum_{i=1}^{n}(v_i - v_a)^2}}{v_a} \quad (1)$$

where n is the number of measuring points on the same section; v_i is the flow velocity at the measuring point; and v_a is the average flow velocity at the cross-section.

Figure 6 shows the variation curves of turbulence intensity at different filling degrees for each cross-section.

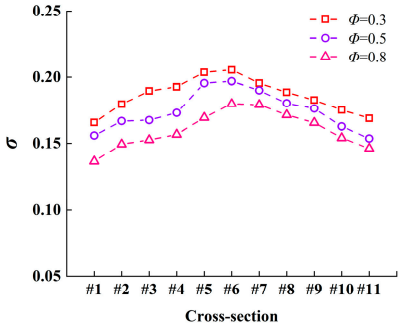


Figure 6. Turbulence intensity of each section of the main channel at different filling degrees.

It can be seen that the trend of turbulence intensity in the x-axis direction is the same for different filling degrees, with the turbulence intensity first increasing and then decreasing. In the upstream and downstream areas of the main channel, which are far away from the pipeline, the turbulence intensity of each section is relatively small, and the flow velocity fluctuation is small, showing that the pipeline has a relatively small impact on the water flow in the main channel. Cross-sections #4–#8 face the inlet of the pipeline, and the turbulence intensity of each section is enhanced, resulting in increased water flow fluctuations. As the filling degree increases, the turbulence intensity of each section of the main channel decreases.

Due to the influence of pipeline diversion, the flow velocity in the junction area of the channel and pipe fluctuates greatly. The fluctuation intensity at sections #4, #6, and #8 was studied, and the turbulence intensity of the measuring lines on these three sections is shown in Figure 7.

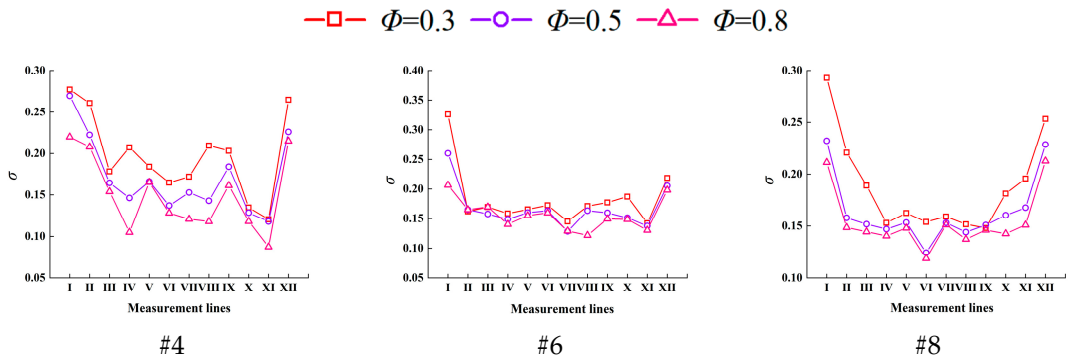


Figure 7. Turbulence intensity of each cross-section measurement line at different filling degrees.

The fluctuation amplitude of the turbulence intensity curve of each section from measurement lines I to XII under different filling degrees is relatively large, as can be

seen from Figure 7. This is mainly due to the fact that at the entrance of the pipeline, the channel flows uniformly, the water in the pipeline flows freely, and the reverse water flows intersect here, resulting in complex water flow patterns and large fluctuations in flow velocity at these three sections, featuring poor regularity. The turbulence intensity on measurement lines I and XII is relatively high, mainly due to the fact that the water flow near the wall of the main channel is greatly affected by wall shear stress, resulting in a large velocity gradient and high turbulence intensity. However, the center position of the main channel further away from the wall is less affected by wall shear stress, and the turbulence of the water flow is suppressed under the action of a viscous force, resulting in a decrease in turbulence intensity. As the filling degree increases, the turbulence intensity of the measuring line gradually decreases.

3.1.3. Analysis of Flow Velocity in a Non-Pressure Pipe

It was found that the flow velocity v of the non-pressure pipe was mainly affected by the flow velocity of the main canal (v_1), the average water depth of the main channel (H), the width of the canal (B), the diameter of the pipeline (D), the depth of the water in the pipeline (h), the distance from the center of the pipeline to the bottom of the canal (c), the density of the liquid (ρ), the viscous coefficient of motion (μ), and gravitational acceleration (g). Therefore, the flow rate of the non-pressure pipe can be written as the following general function:

$$v = f(v_1, H, B, D, h, c, \rho, \mu, g) \tag{2}$$

There are a total of 10 physical quantities in the above equation, of which the number of independent variables is 10. The three physical quantities H, ρ, and g were selected as the basic physical quantities; thus, Equation (2) could be expressed as a relation composed of numbers of seven dimensions and one dimension. According to the π theorem, Equation (2) can be expressed as follows:

$$\frac{v}{\sqrt{gH}} = f\left(\frac{v_1}{\sqrt{gH}}, \frac{h}{H}, \frac{B}{H}, \frac{D}{H}, \frac{c}{H}, \frac{\mu}{H\sqrt{gH}}\right) \tag{3}$$

Equation (3) can be further translated into the following form:

$$v = f\left(Fr, \frac{h}{H}, \frac{B}{H}, \frac{D}{H}, \frac{c}{H}, Re\right)\sqrt{gH} \tag{4}$$

Here, Fr is the Froude number of the main canal; h/H is the water depth ratio of the pipeline to the channel; B/H is the width/depth ratio of the channel width to the water depth of the main channel; D/H is a ratio of the diameter of the pipe to the water depth of the main channel; c/H is the buried depth ratio, corresponding to the depth from the center of the pipeline to the bottom of the canal to the water depth of the main channel; and Re is the Reynolds number. Equation (4) can be simplified to the following form:

$$v = \varphi\sqrt{gH} \tag{5}$$

Here, φ is the flow velocity coefficient of the non-full pipe, which is a variable related to factors such as the Froude number, water depth ratio, width/depth ratio, diameter/depth ratio, buried depth ratio, Reynolds number, and other factors. In this test, because channel width, pipe diameter, and the center position of the pipe are all fixed values, and the range of Reynolds number (Re) values is 16,419~44,668, the type of water flow is turbulent flow, and the influence of viscous force is much less than that of inertial force; therefore, the above factors can be ignored, and φ can be expressed as follows:

$$\varphi = f\left(Fr, \frac{h}{H}\right) \tag{6}$$

It can be gleaned from Equation (6) that the flow velocity coefficient of the non-pressure pipe is related to Fr and h/H. In order to study the relationship between the flow velocity coefficient of the non-pressure pipe and the above factors, the variation curve of the flow velocity coefficient of the non-pressure pipe under different influencing factors was determined according to the test results, as shown in Figure 8.

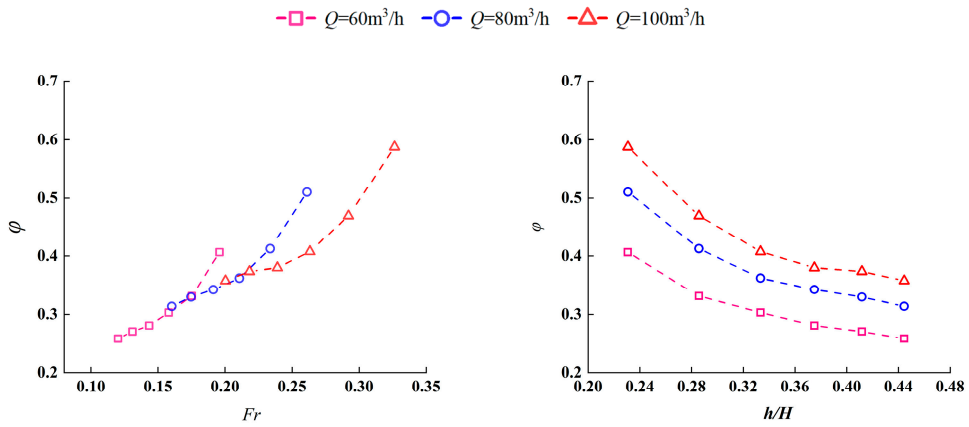


Figure 8. Relationship between various factors and velocity coefficient: (**a**) Fr and φ relationship; (**b**) h/H and φ relationship.

Figure 8 shows that when the flow rate is constant, the flow velocity coefficient of the non-pressure pipeline increases with the increase in Fr and decreases with the increase in h/H. This is mainly due to the fact that the changes in Fr and h/H are directly related to the depth of the water in the main channel, and when the water depth of the main channel decreases, Fr and h/H decrease. According to Equation (5), it can be seen that when the pipeline flow velocity increases and the water depth decreases, the flow velocity coefficient increases, and then the pipeline flow velocity coefficient increases with the increase in main channel Fr and decreases with the increase in h/H.

In order to quantitatively analyze the relationship between the flow velocity coefficient of the non-pressure pipeline and Fr and h/H, an expression depicting the flow velocity coefficient of the non-pressure pipeline was obtained via linear regression analysis, as shown in Equation (7).

$$\varphi = 1.19Fr - 0.277h/H + 0.224 \quad (7)$$

In order to verify the accuracy of Equation (7), the calculated results were compared with the test results, as shown in Table 2.

Table 2. Comparison between calculated and measured values of the flow velocity coefficient.

Φ	Q (m^3/h)	Observed Values	Calculated Value	Relative Error (%)
0.3	50	0.38	0.35	6.22
	70	0.47	0.43	7.73
	90	0.56	0.51	8.75
	110	0.62	0.59	4.52
0.5	50	0.30	0.29	5.33
	70	0.33	0.35	7.93
	90	0.39	0.41	7.03
	110	0.43	0.47	8.57
0.8	50	0.24	0.22	8.81
	70	0.28	0.27	5.33
	90	0.34	0.32	5.97
	110	0.38	0.36	4.74

The maximum relative error between the calculated and measured values of the non-pressure pipe velocity coefficient is 8.81%, indicating that it is feasible to use Formula (7) to calculate the non-pressure pipe velocity coefficient. At the same filling degree, as the flow rate of the main channel increases, the non-pressure pipe velocity coefficient increases. This is mainly because when the filling degree is constant, the water depth in the main channel also remains unchanged, and as the flow rate of the main channel increases, the flow velocity of the water entering the pipeline also increases, and the velocity coefficient increases according to Formula (5). At the same main channel flow rate, as the filling degree increases, the non-pressure pipe flow velocity coefficient decreases. This is mainly because when the main channel flow rate is constant, the depth of water in the main channel increases with the increase in the filling degree, and the main channel flow velocity decreases with the increase in the filling degree. The flow velocity of the water entering the pipeline also decreases, and the non-pressure pipe flow velocity coefficient decreases according to Formula (5).

3.2. Analysis of the Water Surface of the Main Channel

According to the test results, we created a schematic diagram of the changes to the water surface of the main canal at different filling degrees, as shown in Figure 9.

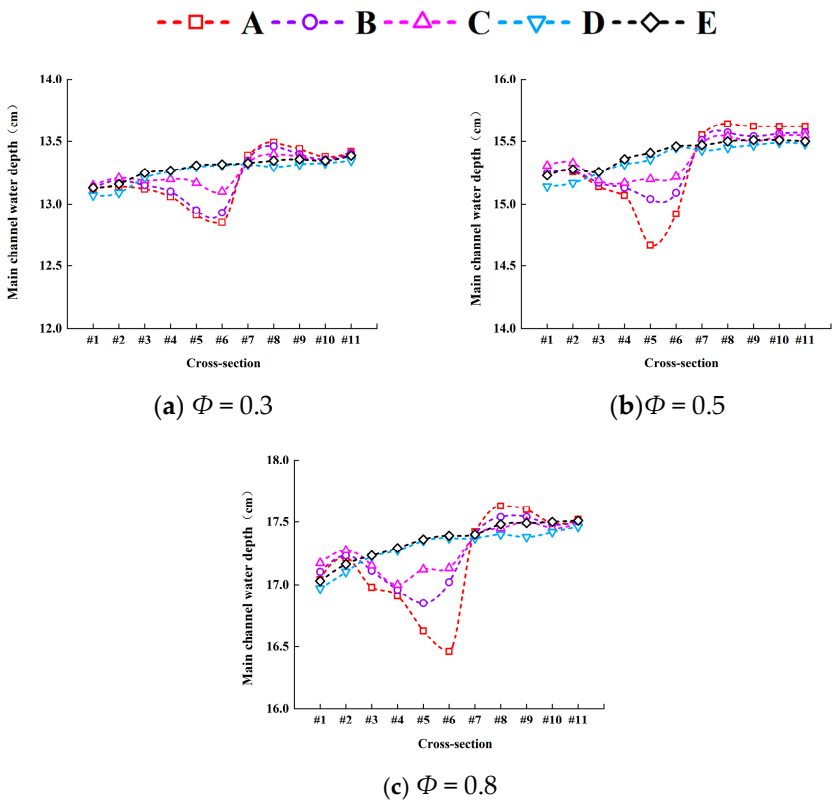


Figure 9. Water surface at different filling levels.

Evidently, the trend of the water surface of the main channel along the *x*-axis is roughly the same at different filling degrees. Water surface measurement lines A to C are relatively close to the entrance of the pipeline and the wall of the main channel, and the water surface measurement lines fluctuate greatly along the *x*-axis, forming a "V" shape. The flow state of the water at sections #1 and #2 is relatively stable, with a slight increase in the height of the water surface. Starting from section #3, the water flow velocity on one side of the main channel wall where the pipeline is located gradually increases along the *x*-axis, the kinetic energy of the water flow increases, the potential energy decreases, and the height of the water surface decreases. The water flow velocity reaches its maximum near section #6. The potential energy is minimized, and the water surface height drops to its lowest point.

Sections #7 to #9 are subjected to the action of reverse water flow, resulting in a decrease in flow velocity and an increase in water surface height. In addition, the blocking effect of the pipeline wall further raises the water level of sections #7 to #9, causing a significant increase in water surface height. During the experiment, the water surface changes at the inlet of the pipeline could be clearly observed, as shown in Figure 10. For water surface measurement lines D and E, due to the relatively small influence of pipelines, the fluctuation in water surface height is small; the height of the water's surface gradually rises as it flows. In the upstream and downstream areas of the main channel, which are less affected by pipelines, the water surface shows a trend of being lower in the middle and higher on both sides in the *y*-axis direction, and the water depths near the walls on both sides are not significantly different. In the area facing the entrance of the pipeline, the water surface shows a gradually increasing trend in the *y*-axis direction.

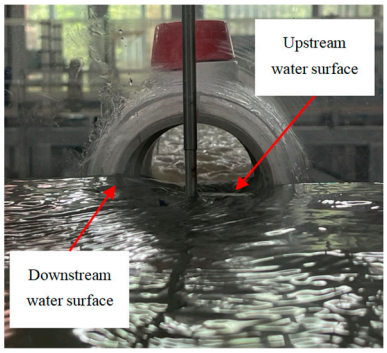


Figure 10. Water surface at the inlet of the pipeline.

3.3. Analysis of Flow Distribution in Channel–Pipe Combined Irrigation Systems

3.3.1. Water Diversion Width

When the water flowing in the main channel approaches the diversion outlet, some of the water flows away from the main stream and is diverted into the pipeline, while the rest continues to flow downstream. At this time, the diverted water flow forms a separation surface with the main stream, and the vertical distance from the starting point of the diverted water flow to the wall of the main channel is called the diversion width. The size of the water diversion width affects the degree of water diversion and the distribution of sediment movement. Therefore, in this study, we examined the water-splitting width at different water depths at different filling degrees. Based on the relevant experimental results, we created velocity vector diagrams for different water depths at different filling levels, as shown in Figure 11.

The curved red line in Figure 11 is the boundary line for water diversion width. The upstream flow begins to divert from this position between sections #1 and #2. The closer one moves to the water diversion point, the greater the curvature of the water flow. The curvature reaches a maximum at the lower edge of the pipeline, and with the increase in the filling degree, the curvature of the water-splitting width curve also increases. Due to the influence generated by the diversion of water from the pipeline, the water around the water diversion point has a tendency to flow into the pipeline, resulting in a small area of reverse flow near the lower edge of the pipeline. When the filling degrees are 0.3 and 0.5, the water diversion width increases from the bottom of the pipe to the upper layer; that is, the closer we move toward the water surface, the greater the water diversion width. When the filling degree is 0.8, the water diversion width increases first and then decreases from the bottom of the pipe to the upper layer. This is mainly because for the circular section, when the filling degree is less than 0.5 (i.e., the water depth is less than the radius), as the water depth increases, the upper water inlet width of the pipeline becomes greater than the width at the bottom, and more water flows into the water inlet, making the upper water inlet width greater than that of the bottom. When the filling degree is greater than 0.5 (i.e., the water depth is greater than the radius), with the increase in water depth, the

width of the last water inlet gradually becomes smaller, while the width of the water inlet at the center of the pipeline becomes the largest, making the width of the water diversion at the bottom and upper layers smaller than that in the middle of the pipeline, so the width of the diverted water stream from the bottom of the pipeline to the upper layer shows a trend of increasing first and then decreasing. Through calculation, we determined that when the filling degrees are 0.3, 0.5, and 0.8, the water distribution width from the bottom to the surface is between approximately 3.2 and 4 cm, 4.3 and 6 cm, and 7.3 and 11 cm. Evidently, with the increase in the filling degree, the water distribution width increases, and the increase in water distribution width when the filling degree increases from 0.5 to 0.8 is greater than that when the filling degree increases from 0.3 to 0.5.

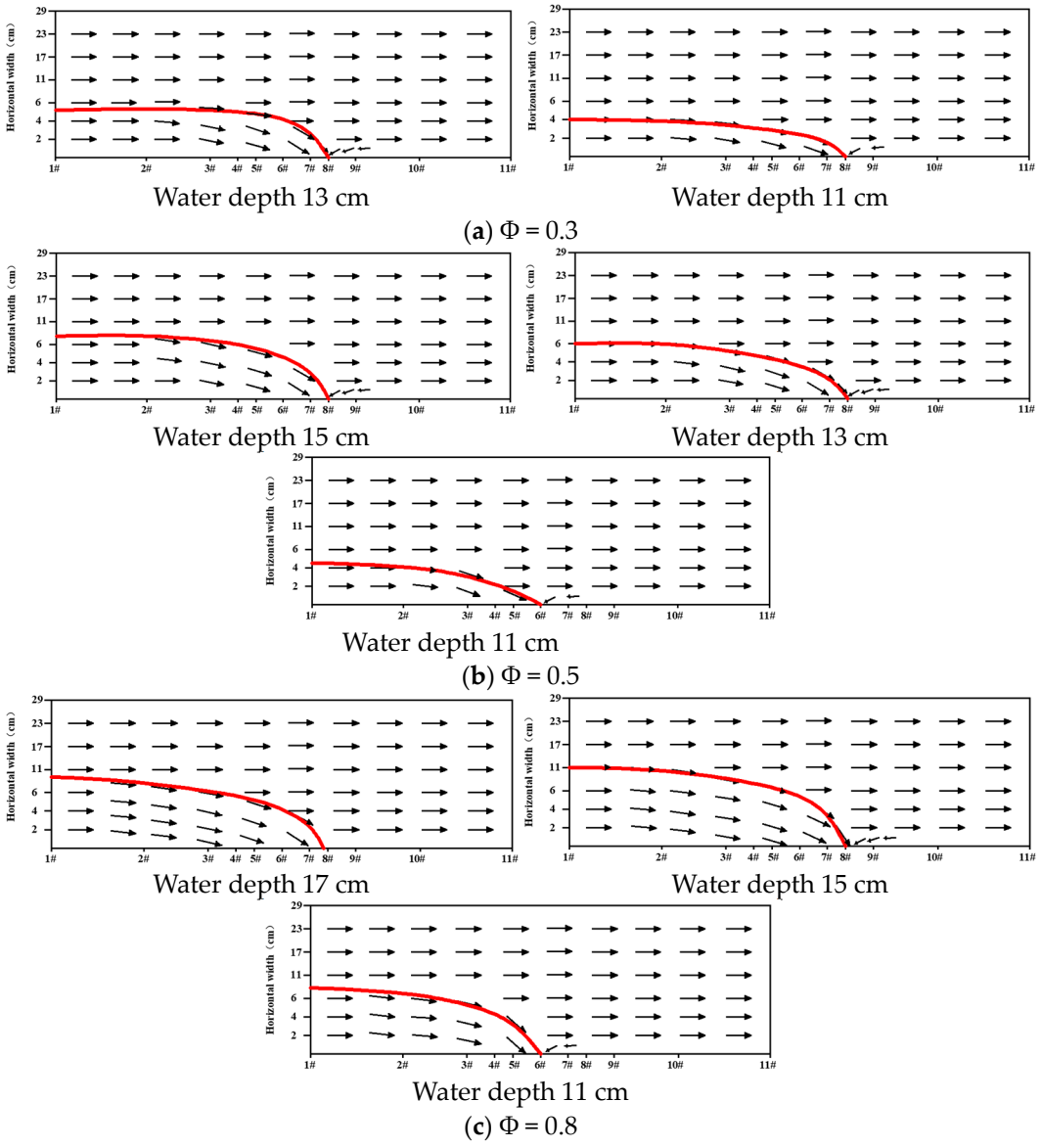


Figure 11. Velocity vector diagram at different depths of water at different filling degrees. Note: The red line represents the boundary line for water diversion width.

3.3.2. Diversion Ratio

The ratio of pipeline flow Q_p to main channel flow Q is known as the diversion ratio δ; that is, $\delta = Q_p/Q$. Table 3 shows the pipeline diversion ratio at different filling degrees.

Table 3. Diversion ratio under different working conditions.

Φ	Q (m^3/h)	Q_p (m^3/h)	Diversion Ratio (%)
0.3	50	3.08	6.16
	70	3.77	5.38
	90	4.50	5.00
	110	4.95	4.5
0.5	50	4.86	9.72
	70	5.57	7.96
	90	6.63	7.36
	110	7.43	6.75
0.8	50	7.80	15.60
	70	9.11	13.02
	90	10.81	12.01
	110	12.38	11.16

When the filling degree is constant, as the flow in the main channel increases, the flow in the pipeline also gradually increases, while the diversion ratio gradually decreases. This is mainly because when the filling degree is constant, the depth of water in the main channel remains unchanged, the flow rate of the main channel increases, the flow velocity of the water increases, and the flow velocity of the water entering the pipeline also increases. When the cross-section of the pipeline remains unchanged, the flow rate of the pipeline increases. It can be seen that for every 20 m^3/h increase in the flow in the main channel, the maximum increase in pipeline flow is 1.57 m^3/h, which means that the growth rate of pipeline flow in this experiment is lower than that of the main channel flow, resulting in a decrease in the diversion ratio. When the main channel flow rate is constant, as the filling degree increases, the pipeline flow rate increases and the diversion ratio increases. This is mainly because when the flow rate of the main channel is constant, as the filling degree increases, the depth of water in the main channel increases, the water flow velocity of the main channel decreases, the inertial force of main channel water flow decreases, and the main channel water flow is more easily diverted into the pipeline. Although the decrease in the flow velocity of the main channel reduces the flow velocity of the water entering the pipeline, the cross-sectional area of the pipeline increases with the increase in the filling degree. In this experiment, the growth rate of the water flow cross-section of the pipeline was greater than the rate of decrease in the water flow velocity in the pipeline, resulting in a gradual increase in the flow rate inside the pipeline, and the corresponding diversion ratio also increased accordingly. When the filling degree increased from 0.3 to 0.5, the increase in pipeline flow was between approximately 1.78 and 2.48 m^3/h. When the filling degree increased from 0.5 to 0.8, the increase in pipeline flow was between approximately 2.94 and 4.95 m^3/h. It can be gleaned that when the filling degree is less than 0.5 (i.e., the water depth is less than the pipe radius), the increase in pipeline flow is small when the filling degree increases. When the filling degree is greater than 0.5 (i.e., the water depth is greater than the pipe radius), the increase in pipeline flow is greater with the increase in the filling degree, which corresponds to the change rule of water distribution width with respect to the filling degree.

4. Discussion

With the acceleration of the modernization of irrigation areas, the gradual realization of the water transmission mode wherein channels are replaced with pipes has become the main direction for the development of irrigation areas. Yet, due to the influence of various factors, it is unrealistic to completely replace channels with pipelines. The side pipes in channel–pipe combined irrigation systems can be regarded as a kind of circular section of the "side channel". It has also been found that the influence of the pipeline on the flow velocity and water surface change along the main channel is similar to the influence of rectangular and trapezoidal side channels. Therefore, the research results concerning

rectangular and trapezoidal side channels can be referred to when studying the hydraulic characteristics of channel–pipe combined irrigation systems.

This article reflects the flow velocity fluctuation states of each section and measurement line through turbulence intensity and reveals the impact range of non-pressure pipe flow on main channel water flow as determined through combining flow velocity changes and diversion width. Through dimensional analysis, an expression of the flow velocity of non-pressure pipe flow in channel–pipe combined irrigation systems was obtained, and the linear regression analysis method was used to fit the formula of the flow velocity coefficient of non-pressure pipe flow. The value calculated using the formula was compared with the observed value to verify the formula's accuracy. In practical engineering, because pipelines are buried underground, it is difficult to determine the flow velocity of non-pressure pipes. The formula obtained in this study only requires the Froude number and water depth value of the main channel and can be used to quickly calculate the flow velocity of non-pressure pipes, allowing the above problems to be solved quickly and effectively. In this paper, the diversion ratio was also studied, and the relationship between the filling degree and the pipeline flow was derived. The diversion ratio of non-pressure pipe flow increases with the increase in the filling degree. In practical work, when the filling degree of the pipeline is low, the water depth in the main channel can be increased by adjusting the downstream gate, thereby increasing the filling degree of the pipeline and generating a larger pipeline flow rate so as to provide sufficient water for field irrigation.

Unlike how the rectangular water diversion width gradually increases from the water surface to the bottom, the change law of the water diversion width of non-pressure pipes in the water depth direction is more complicated, and the original water diversion width formula is no longer applicable to non-pressure pipe flow. Therefore, conducting further research on the formula for water diversion width has become a new research direction. The main variable of this study is the filling degree, and other factors affecting channel–pipe combined irrigation systems, such as pipeline diameter and pre-buried depth, have not been discussed in depth. Thus, the conclusions obtained have certain limitations. Therefore, it would be useful to analyze the influence of other factors on the hydraulic characteristics of channel–pipe combined irrigation systems under non-pressure pipe conditions. Through follow-up studies, the theoretical system of channel–pipe combined irrigation systems can be improved, and better technical support can be provided for practical application in projects.

5. Conclusions

(1) The turbulence intensity and water surface variation trend are the same at different filling levels. The turbulence intensity shows a trend of first increasing and then decreasing along the pipeline, while the water surface closer to the pipeline shows a trend of first decreasing, then increasing, and finally decreasing. The influence range of non-pressure pipe flow on the water flow of the main channel is about 2 times the longitudinal diameter and 1.5 times the diameter of the pipe from the center of the pipeline.

(2) When the filling degree is constant, with an increase in the flow rate of the main channel, the flow velocity coefficient of the non-pressure pipe increases. When the flow rate of the main channel is constant, the flow velocity coefficient of the non-pressure pipe increases with an increase in the Froude number of the main channel and decreases with an increase in the water depth ratio, and the maximum relative error between the calculated value and the measured value does not exceed 8.81%.

(3) The width of water diversion increases with an increase in the filling degree. When the filling degree is less than 0.5, the width of water diversion decreases gradually from the water surface to the bottom. When the filling degree is greater than 0.5, the width of water diversion increases first and then decreases from the water surface to the bottom.

(4) The diversion ratio of non-pressure pipe flow decreases with an increase in the flow rate and increases with an increase in the filling degree. Therefore, in the actual process of supplying water to a field, when the inflow of the main channel is constant, the water

depth in the main channel can be changed to increase pipeline diversion and improve pipeline flow.

Author Contributions: Conceptualization, X.J.; methodology, X.J.; validation, Y.S. (Yuqi Shen) and Y.S. (Yi Sun); formal analysis, X.J.; investigation, X.J., W.Z. and Y.W.; writing—original draft preparation, X.J.; writing—review and editing, X.J. All authors have read and agreed to the published version of the manuscript.

Funding: This research was funded by the Central Public-interest Scientific Institution Basal Research Fund, grant number IFI2023-10, IFI2024-10, and the Henan Provincial Key R&D and Promotion Special-Science and Technology Tackling Project, project number 232102110290.

Data Availability Statement: The data that support this study will be shared by the corresponding author upon reasonable request. The data are not publicly available because they are being used in an ongoing investigation and experiment.

Conflicts of Interest: The authors declare no conflicts of interest.

References

1. Liao, X.H. Present Situation and Improvement Measures of Agricultural Water and Soil Engineering in China. *Agri. Eng.* **2017**, *7*, 113–114.
2. Han, Z.Z. Prospective Development of Irrigation Districts and Technology Innovation. *China Rural Water Hydropower* **2016**, *8*, 1–3.
3. Xu, C.F.; Gao, J.D.; Zhang, D.Q. Experimental Study on the Flow Distribution in a Low-pressure Multi-outlet Irrigation Pipeline System. *J. Irrig. Drain.* **2020**, *39*, 96–100.
4. Montaseri, H.; Asiaei, H.; Baghlani, A. Numerical study of flow pattern around lateral intake in a curved channel. *Int. J. Mod. Phys. C* **2019**, *30*, 1950083. [CrossRef]
5. Ahmadi, F.; Ebrahimian, M.; Sanders, R.S. Particle image and tracking velocimetry of solid-liquid turbulence in a horizontal channel flow. *Int. J. Multiphas. Flow* **2019**, *112*, 83–99. [CrossRef]
6. Jin, H.Z.; Yan, H.J.; Qian, Y.C. Overseas Development of Water saving Irrigation Engineering Technology. *Trans. Chin. Soc. Agric. Mach.* **2010**, *41*, 59–63.
7. Nedelec, Y.; Gay, B. Experimental study of a right-angled end junction between a pipe and an open channel. *J. Hydraul. Eng.* **2008**, *134*, 616–625. [CrossRef]
8. Li, Z.W.; Wang, X.F.; Xiong, J.Y. Flow structure of the confluence between an open channel and a pipe. *Water Sci. Technol.* **2023**, *88*, 2646–2660. [CrossRef]
9. Li, Z.W.; Wang, X.F.; Xiong, J.Y. Flow structure, bed morphology and contaminated sediment transport at the confluences of pipe and channel. *Environ. Fluid Mech.* **2024**, *24*, 367–385. [CrossRef]
10. Barkdoll, B.D.; Odgaard, A.J.; Hagen, B.L. Experimental comparison of dividing open-channel with duct flow in T-junction. *J. Hydraul. Eng.* **1998**, *124*, 92–95. [CrossRef]
11. Sharabian, N.M.; Karakouzian, M.; Hayes, D. Flow Topology in the Confluence of an Open Channel with Lateral Drainage Pipe. *Hydrology* **2020**, *7*, 57. [CrossRef]
12. Alandi, P.P.; Alvarez, O.J.; Martin-Benito, T.J. Optimization of irrigation water distribution networks, layout included. *Agr. Water Manag.* **2007**, *88*, 110–118. [CrossRef]
13. Lorente, S.; Wechsatol, W.; Bejan, A. Tree-shaped flow structures designed by minimizing path lengths. *Int. J. Heat Mass Trans.* **2002**, *45*, 3299–3312. [CrossRef]
14. Li, Y.; Zhang, J.; Bai, Y.C. Experimental study on characteristics of fluctuating pressure in sediment flow pipeline. *J. Hydraul. Eng.* **2020**, *51*, 967–978.
15. Cheng, M.; Sun, F.W.; Zhang, Q.H. Experimental Study on Frictional Drag of Pipeline on Transporting Yellow River's Water in the Lower Reaches of the Yellow River. *J. Irrig. Drain.* **2015**, *34*, 3–36.
16. Zhao, L.L.; Lai, Z.Q.; Wang, Z.M. A Review of Fluid and Coarse Particle Hydraulic Conveying in the Pipe. *China Rural Water Hydropower* **2022**, *10*, 182–189.
17. Liu, J. Discussion on the Development Mode of Pipeline Irrigation Technology in Canal Irrigation Area. *Sanxi Water Sci. Tech.* **2019**, *4*, 91–92.
18. Adigamov, R.R.; Andreev, V.A.; Rogachev, S.O. Effect of Pipe Forming on the Mechanical Properties of Large Diameter Pipes. *Russ. Metall.* **2023**, *2023*, 498–507. [CrossRef]
19. Cunliffe, C.J.; Dodds, J.M.; Dennis, D.J.C. Flow correlations and transport behaviour of turbulent slurries in partially filled pipes. *Chem. Eng. Sci.* **2021**, *235*, 116465. [CrossRef]
20. Ding, F.L.; Mao, Z.Y. Hydraulic characteristics of partially-filled flow in circular pipe. *Adv. Water Sci.* **2020**, *4*, 547–555.
21. Berlamont, E.J.; Trouw, K.; Luyckx, G. Shear Stress Distribution in Partially Filled Pipes. *J. Hydraul. Eng.* **2003**, *129*, 697–705. [CrossRef]
22. Davis, S.D. Nomograph for Flow from Partially Filled Pipes. *Ind. Eng. Chem.* **2002**, *34*, 52. [CrossRef]

23. White, F.M. *Fluid Mechanics*, 4th ed.; McGraw Hill Higher Education: Boston, MA, USA, 1999; p. 659.
24. Knight, D.W.; Sterling, M. Boundary shear in circular pipes running partially full. *J. Hydraul. Eng.* **2000**, *126*, 263–275. [CrossRef]
25. Yoon, J.I.; Sung, J.; Lee, M.H. Velocity profiles and friction coefficients in circular open channels. *J. Hydraul. Res.* **2012**, *50*, 304–311. [CrossRef]
26. Jiang, Y.; Li, B.; Chen, J. Analysis of the velocity distribution in partially-filled circular pipe employing the principle of maximum entropy. *PLoS ONE* **2016**, *11*, 151–163. [CrossRef] [PubMed]
27. Mohamed, E.; Ahmed, S. Explicit Solution for the Specific Flow Depths in Partially Filled Pipes. *J. Pipeline Syst. Eng.* **2017**, *8*, 06017004.
28. Mao, Z.Y.; Zhao, X.; Luo, S. Analytic expression for partially -filled flow velocity in pipe of circular section. *Adv. Water Sci.* **2007**, *18*, 170–174.
29. Ding, F.L.; Mao, Z.Y.; Han, K. Establishment of velocity function of partially-filled flow in circular pipe based on simulation and physical model experiment. *Trans. Chin. Soc. Agricul. Eng.* **2019**, *35*, 55–61.

Disclaimer/Publisher's Note: The statements, opinions and data contained in all publications are solely those of the individual author(s) and contributor(s) and not of MDPI and/or the editor(s). MDPI and/or the editor(s) disclaim responsibility for any injury to people or property resulting from any ideas, methods, instructions or products referred to in the content.